

PAPER

The role of spatial structures of tissues in cancer initiation dynamics

To cite this article: Cade Spaulding *et al* 2022 *Phys. Biol.* **19** 056003

View the [article online](#) for updates and enhancements.

You may also like

- [Laser-assisted 3D bioprinting of exocrine pancreas spheroid models for cancer initiation study](#)
Davit Hakobyan, Chantal Médina, Nathalie Dusserre et al.

- [Stochastic dynamics of cancer initiation](#)
Jasmine Foo, Kevin Leder and Franziska Michor

- [The matrix environmental and cell mechanical properties regulate cell migration and contribute to the invasive phenotype of cancer cells](#)
Claudia Tanja Mierke



IOP | ebooks™

Bringing together innovative digital publishing with leading authors from the global scientific community.

Start exploring the collection—download the first chapter of every title for free.

Physical Biology



PAPER

The role of spatial structures of tissues in cancer initiation dynamics

RECEIVED
19 May 2022

REVISED
11 July 2022

ACCEPTED FOR PUBLICATION
28 July 2022

PUBLISHED
18 August 2022

Cade Spaulding¹, Hamid Teimouri^{1,2} and Anatoly B Kolomeisky^{1,2,3,4,*}

¹ Department of Chemistry, Rice University, Houston, TX 77005-1892, United States of America

² Center for Theoretical Biological Physics, Rice University, Houston, TX 77005-1892, United States of America

³ Department of Chemical and Biomolecular Engineering, Rice University, Houston, TX 77005-1892, United States of America

⁴ Department of Physics and Astronomy, Rice University, Houston, TX 77005-1892, United States of America

* Author to whom any correspondence should be addressed.

E-mail: tolya@rice.edu

Keywords: cancer initiation dynamics, stochastic models, Moran processes, evolutionary dynamics

Supplementary material for this article is available [online](#)

Abstract

It is widely believed that biological tissues evolved to lower the risks of cancer development. One of the specific ways to minimize the chances of tumor formation comes from proper spatial organization of tissues. However, the microscopic mechanisms of underlying processes remain not fully understood. We present a theoretical investigation on the role of spatial structures in cancer initiation dynamics. In our approach, the dynamics of single mutation fixations are analyzed using analytical calculations and computer simulations by mapping them to Moran processes on graphs with different connectivity that mimic various spatial structures. It is found that while the fixation probability is not affected by modifying the spatial structures of the tissues, the fixation times can change dramatically. The slowest dynamics is observed in ‘quasi-one-dimensional’ structures, while the fastest dynamics is observed in ‘quasi-three-dimensional’ structures. Theoretical calculations also suggest that there is a critical value of the degree of graph connectivity, which mimics the spatial dimension of the tissue structure, above which the spatial structure of the tissue has no effect on the mutation fixation dynamics. An effective discrete-state stochastic model of cancer initiation is utilized to explain our theoretical results and predictions. Our theoretical analysis clarifies some important aspects on the role of the tissue spatial structures in the cancer initiation processes.

Cancer remains one of the most serious health problems in our society [1]. It is well known that tumor formation is the result of uncontrolled division of malfunctioning cells that harbor several types of genetic or epigenetic alterations, which, in turn, are caused by intrinsic errors during DNA replication and repair as well as by some other external factors [1–5]. Cancer can strike any part of the body, but the probability of being diagnosed with a specific type of cancer wildly varies for different types of tissues [6, 7]. It is now strongly believed that tissues have evolved to minimize the risk of tumor formation in them [8–12]. Specific spatial cellular organization of tissues has been proposed as a possible pathway to achieve this goal, although the mechanisms of underlying microscopic processes remain not well understood [8, 10, 13, 14].

There are multiple theoretical investigations on microscopic mechanisms of cancer initiation that utilized a wide spectrum of mathematical methods and approaches [15–24]. The majority of them, however, consider tissues as structureless well-mixed homogeneous cellular medium, thus ignoring the spatial organization and cellular heterogeneity. In addition, most of these studies concentrated on probabilities of mutation fixation as indicators of the appearance of tumors [25], while the dynamics of cancer initiation has been rarely explored in theoretical investigations [22–24]. It is important to note that cancer initiation should be characterized by at least two quantities: (1) cancer life-time risk, which is proportional to the mutation fixation probability; and (2) cancer initiation time, which can be approximated by the mutation fixation times. The knowledge of these two

properties should provide a quantitative measure of the danger of developing the tumor [22–24].

To better understand the heterogeneity of cells and interactions during the formation of tumors in tissues, the method that considers evolutionary dynamics on graphs has been introduced in 2005 [26]. The main idea here is that every cell can be viewed as a node on graph, and specific changes in the given cell can stimulate other changes only in cells connected to the original one. Using this approach, it was shown that the topology of the graph might have a dramatic effect on the establishment of new mutants in various cell populations [26–28] and on the rate of evolution [29]. The application of evolutionary dynamics on graphs for somatic evolution in multi-cellular organisms also suggested that certain tissue structures could minimize the onset of cancer [8, 26]. In addition, it was found that some tissue structures might serve as amplifiers of selection, i.e., they might increase the fixation probability of advantageous mutations, while decreasing the fixation probability of disadvantageous mutations [30]. However, a majority of previous studies of evolutionary dynamics on graphs investigated only the fixation probability as a primary characteristic of cancer initiation [25]. Yet, a comprehensive understanding of the role of spatial structures in cancer initiation requires analyzing fixation times as well [31].

In this paper, we present a theoretical investigation of cancer initiation dynamics for tissues with different spatial structures. In our approach, we utilize the evolutionary dynamics on graphs with different connectivity that mimics the changes in the tissue spatial structures. We introduce a connectivity parameter that provides a quantitative measure for describing different spatial structures. An effective discrete-state stochastic description of the cancer initiation process is developed. This allows us to explicitly evaluate the fixation times and the fixation probabilities using a method of first-passage probabilities. Our theoretical calculations suggest that for homogeneous cellular tissues varying the spatial structures does not affect the fixation probabilities, while the fixation times can be strongly modified. The theoretical model explicitly proposes that the risk of the cancer can be lowered by significantly delaying the onset of tumor formation via properly modifying the spatial structures of the tissue.

1. Theoretical method

Let us consider a tissue compartment with originally N normal stem cells that can divide and disappear while keeping the total number of cells constant to reflect a homeostasis that is observed in healthy tissues [1, 3, 24]. Please note that tissues typically also have other non-stem cell, known as progenitor cells, that can differentiate only few times. In contrast, stem cells can differentiate indefinitely. These progenitor cells

do not participate in homeostatic equilibrium, and most probably they are less relevant for the tumor formation. For this reason, in our theoretical analysis we do not take them into account.

To better understand the role of spatial structures, we consider two specific examples of tissues with different structures, as shown in figure 1. In the first case, the tissue can be organized as a one dimensional chain in which each cell can influence only its two nearest-neighbor cells: see figure 1(a). However, in a different arrangement of cells, which can be viewed as effectively two-dimensional sheet as shown in figure 1(b), each cell can influence four of its nearest-neighbor cells. Now, let us assume that a single cell becomes mutated (shown in red in figure 1), and it can divide faster than the normal wild-type cells (shown in green in figure 1). An important difference between the two structural arrangements is that in the one-dimensional tissue the offspring of the mutated cell can replace one of the two neighbors (shown in yellow in figure 1). However, for the two-dimensional tissue, because the mutated cell is connected to four neighbors, its offspring can replace four cells. Multiple other tissue spatial structures might be realized. One may ask then the following questions: in which spatial configuration the fixation probability of the mutated cell is higher? Which structures would also lead to faster fixation dynamics of the mutated cells and why?

To answer these questions and to understand better the role of tissue spatial structures in lowering the risk of cancer development, we consider a theoretical model presented in figure 2(a). There are N stem cells in the tissue that can be viewed as nodes in a directed graph. Before cancer strikes the tissue, the system is in homeostasis, which means that the total number of stem cells is always fixed [15, 24]. Each cell is connected to its l ($l = 1, 2, \dots, N - 1$) neighbors. To describe the evolutionary dynamics in the system, we adopt a Moran process on graphs [26]. This means that if the i th cell is replicated, then with the probability $1/l$ one of the cells from $i + 1$ to $i + l$ will be immediately removed to keep the total number of cells in the tissue constant: see figure 2(a). In our theoretical approach, the homogeneous tissue is viewed as a directed graph where links identify possible changes (cell removals) that might happen after the cell divisions.

It is important to note that in our model all cells are identical and have the same connectivity. One can see that the parameter l reflects the local spatial structure of the real tissue. Then changing the value of l but keeping the same topology of the graph and the same total number of cells provides a convenient way to *quantitatively* probe the effect of spatial structures. This is the main idea of our theoretical approach. Here topology means a specific symmetry of the directed graph. In this paper, we only consider the graphs where all nodes are identical, but other graph

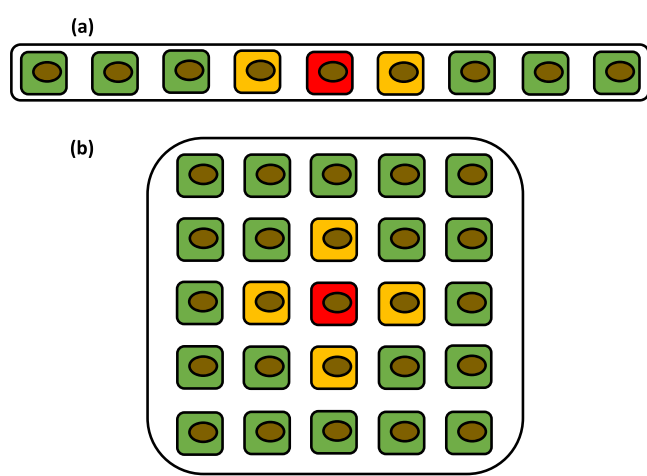


Figure 1. A schematic illustration of the spatial organization of cell populations in tissues. For each structure, all individual cells have the same number of neighbors. Red cells indicate the cells with mutations, yellow cells describe the cells that might be affected soon because they are the neighbors of already mutated cells, and green cells are those where changes are not happening at the given moment. (a) Cells are arranged as a one-dimensional system such that each cell has at most two nearest neighbors. (b) Cells are arranged as a two-dimensional system such that each cell has at most four nearest neighbors.

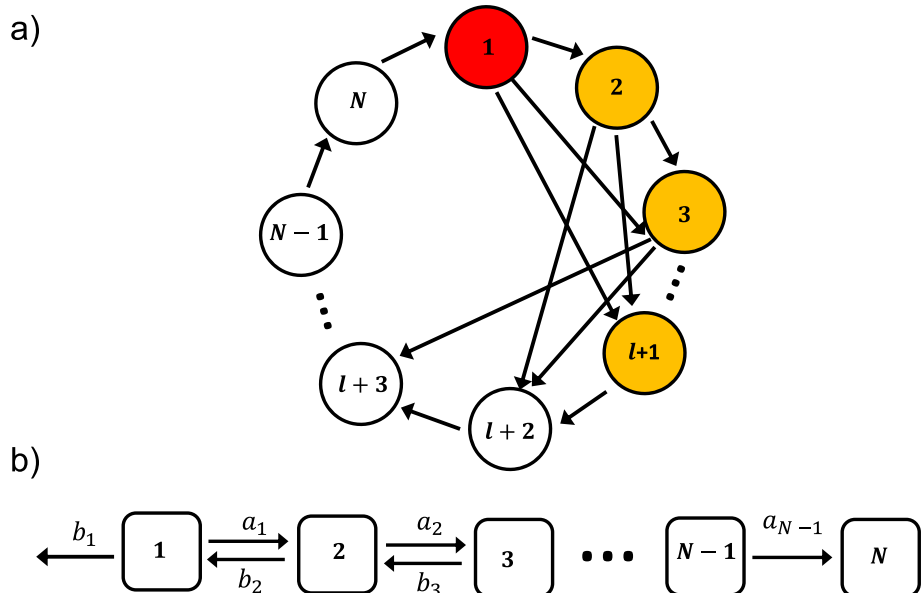


Figure 2. (a) Schematic view of tissue as a directed graph where cells are the nodes and arrows show the directions of possible cell removals after the replication at the given cell. The mutation at site 1 (red circle) will affect one of l sites $2, \dots, l + 1$ that are shown as yellow circles. (b) Corresponding discrete-state stochastic model of evolutionary dynamics for a single mutation fixation in the system.

symmetries can also be investigated. In addition, it can be concluded that the model with $l = 1$ describes an effective one-dimensional tissue structure, while the models with $l = N - 1$ or $l = N$ (the graph where every cell is connected with another one and with the possibility of self-removal) correspond to well-mixed effectively three-dimensional tissues. Varying the connectivity between $l = 1$ and $l = N$ will allow us to continuously test the cancer initiation dynamics on all possible spatial structures of the tissue.

To investigate the cancer initiation dynamics in the tissues with different spatial structures, we start with a single mutation that is taking place at $t = 0$ at some

randomly chosen cell. Since the mutation rates in real systems are very low [15, 32–34], it is assumed that evolutionary dynamics in the system is accomplished only via stem cells replications and removals with a condition of keeping the total number of cells equal to N at all times. In our model, the normal cells can divide with a rate $b = 1$, while the mutated cells divide with a rate $rb = r$. The parameter r , known as a *fitness parameter*, plays an important role in the cancer initiation dynamics. Since it reflects the overall physiological changes in the mutated cell in comparison with the normal cell, it specifies how faster the mutated cells can replicate in comparison with the normal cells.

Generally, advantageous, neutral and disadvantageous mutations are correspondingly described by $r > 1$, $r = 1$, and $r < 1$. We assume that when all stem cells in the tissue become mutated, which is called a mutation fixation, this corresponds to a tumor formation event and it completes the cancer initiation. As we already discussed above, the tissue compartment may also contain the progenitor cells [35]. But it is assumed in our theoretical approach that they are not participating in the processes that lead to the formation of tumor.

Now we can apply a method of stochastic mapping to obtain a comprehensive description of cancer initiation dynamics [22–24]. The idea here is that at any moment the overall state of the tissue can be specified by a single parameter n that corresponds to having n mutated and $N - n$ normal cells. Then the dynamics in the system can be viewed as a set of stochastic transitions between discrete states of the tissue, as shown in figure 2(b). From the state n the tissue can transform into the state $n + 1$ with a rate a_n , and this corresponds to increasing the number of mutated cells by one. From the state n the tissue can also transition into the state $n - 1$ with a rate b_n , and this corresponds to decreasing the number of mutated cells by one. The tissue might completely remove all mutations: this happens with a rate b_1 from the state 1. When the system reaches the state N (from the state $N - 1$ with a rate a_{N-1}), all cells in the tissue become mutated and this corresponds to the mutation fixation (figure 2(b)).

Mapping the evolutionary dynamics of the tissue to a set of stochastic transitions between discrete states allows us to quantitatively characterize the cancer initiation dynamics by applying a method of first-passage probabilities [22–24]. More specifically, one can introduce a first-passage probability density function $F_n(t)$ that is defined as the probability of reaching the state N (fixation) for the first time at time t if at $t = 0$ the system started in the state n (see figure 2(b)). The temporal evolution of these functions is governed by a set of so-called backward master equations, [36, 37]

$$\frac{dF_n(t)}{dt} = a_n F_{n+1}(t) + b_n F_{n-1}(t) - (a_n + b_n) F_n(t), \quad (1)$$

with initial condition $F_N(t) = \delta(t)$, which means that if we start in the state $n = N$ the fixation is immediately accomplished. As explained above, the parameters a_n and b_n are transition rates between different stochastic states of the system: see figure 2(b). The first-passage probability densities provide a full description of the fixation dynamics. We are interested in two important quantities that characterize the cancer initiation dynamics. The first one is fixation probability which is defined as $\pi_n = \int_0^\infty F_n(t) dt$. Another important property is mean first-passage time, $T_n = \int_0^\infty t F_n(t) dt / \pi_n$, which gives mean fixation time for a mutation.

To obtain explicit expressions for dynamic properties of cancer initiation in tissues with different spatial structures, one has to specify the effective transition rates a_n and b_n between the corresponding discrete states of the system. This can be easily done for small systems. In supporting information (<https://stacks.iop.org/PB/15/056003/mmedia>), we provide exact solutions for cancer initiation dynamics for $N = 3$ and $N = 4$, which are also fully supported by Monte Carlo computer simulations of the corresponding systems. For real biological tissues, however, the number of stem cells is much larger, $N \simeq 10^5 - 10^9$ [6, 38]. While we were not able to solve the model for general values of l and N , analytical results are available for some limiting cases corresponding to $l = 1$, $l = N - 1$ and $l = N$. For intermediate values of the connectivity parameter, $1 < l < N - 1$, we explored Monte Carlo computer simulations to obtain the description of the cancer initiation dynamics.

2. Results and discussion

Let us consider explicitly the limiting cases of tissue structures, which are presented in figure 3, for which full analytical solutions can be obtained, as explained in the supporting information. For $l = 1$, we have a one-dimensional closed chain of cells which is illustrated in figure 3(a). It can be shown that in this case (see the supporting information) the effective transition rates are equal to

$$a_n = r, \quad b_n = 1. \quad (2)$$

Then the fixation probability is given by,

$$\pi_1 = \frac{1 - 1/r}{1 - 1/r^N}. \quad (3)$$

The mean fixation time for the system with $l = 1$ can be explicitly evaluated (see the supporting information), and it is given by

$$T_1(l = 1) = \left[\frac{1 + r^{-N}}{(1 - r^{-N})(r - 1)} \right] N - \frac{1 + r}{(r - 1)^2}. \quad (4)$$

For a very large number of cells in the tissue ($N \rightarrow \infty$) and $r \neq 1$, this expression simplifies into

$$T_1(l = 1) \simeq \frac{N}{|r - 1|}; \quad (5)$$

while for $N \gg 1$ and $r = 1$ we have

$$T_1(r = 1) \simeq \frac{N^2}{6}. \quad (6)$$

These results for the mean fixation times can be explained using the discrete-state stochastic scheme of the cancer initiation process from figure 2(b). For $r \neq 1$, the process can be viewed as a biased random walk with the bias in the direction of the mutation fixation for $r > 1$ (to the right in figure 2(b)) and the

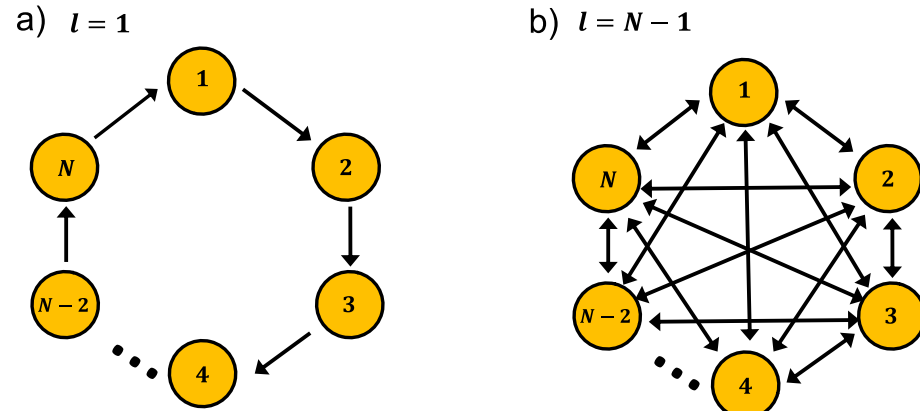


Figure 3. Schematic representations of the stochastic models for cancer initiation dynamics for limiting spatial structures: (a) $l = 1$, and (b) $l = N - 1$.

bias in the direction of the mutation elimination for $r < 1$ (to the left in figure 2(b)). This explains the linear dependence of the mean fixation time on the size of the system since the dynamics can be viewed as a driven motion in the space of discrete cellular tissue states. However, for $r = 1$, the process is an unbiased random walk, leading to quadratic dependence of mean fixation times on the size of the system.

In the opposite limit of high connectivity ($l = N - 1$, which is shown in figure 3(b), and $l = N$), the dynamics of cancer initiation can be also explicitly analyzed. In these cases, we have the following effective transition rates in the corresponding stochastic schemes from figure 2(b), as explained in the supporting information and in reference [22],

$$a_n(l = N - 1) = \frac{rn(N - n)}{N - 1}, \quad (7)$$

$$b_n(l = N - 1) = \frac{n(N - n)}{N - 1},$$

and

$$a_n(l = N) = \frac{rn(N - n)}{N}, \quad b_n(l = N) = \frac{n(N - n)}{N}. \quad (8)$$

One can see that the corresponding transition rates differ only by a constant factor that depends on the size of the system,

$$a_n(l = N) = \frac{N}{N - 1} a_n(l = N - 1), \quad (9)$$

$$b_n(l = N) = \frac{N}{N - 1} b_n(l = N - 1).$$

However, the full Moran process in the well-mixed system ($l = N$) has been already fully investigated [22], allowing us to obtain a comprehensive description of the fixation dynamics in high connectivity limit.

One can easily conclude that the fixation probabilities are the same for $l = N - 1$ and $l = N$, and they also equal to the case for $l = 1$, as given by equation (3). Actually, it can be shown generally

that the fixation probability does not change with varying the spatial structures for homogeneous tissue models [26]. This is our first important result: for homogeneous tissues varying the spatial structures does not decrease the probability of getting the tumor.

The fixation time for the model with $l = N - 1$ is given by [22]

$$T(l = N - 1) = \frac{N + 1}{b} \sum_{n=1}^{N-1} \frac{1}{n(N - n)} \left(\frac{r^n - 1}{r - 1} \right) \times \left(\frac{r^{N-n} - 1}{r^N - 1} \right). \quad (10)$$

In the limit of very large N , it takes the following form [22],

$$T(l = N - 1) \simeq \frac{1}{r(1 - \frac{1}{r^N})} \left[\frac{\text{Ei}(-\ln r)}{\ln r} \left(1 - \frac{1}{r} \right) + \frac{2}{\ln r} (\gamma + \ln [N \ln r]) \right], \quad (11)$$

where $\text{Ei}(x) = -\int_{-x}^{\infty} \frac{e^{-z}}{z} dz$ is the exponential integral, and γ is the Euler–Mascheroni constant.

For intermediate values of the connectivity parameter, $1 < l < N - 1$, we were not able to explicitly determine the transition rates in the discrete-state stochastic description, and for this reason Monte Carlo computer simulations have been utilized to evaluate the fixation mutation dynamics. The results are presented in figure 4. One can see that for the fixed value of the fitness parameter r , increasing the connectivity always lowers the mean fixation times. This can be explained by noticing that there are more pathways to fixation for larger values of l . On each such pathway, the bias to go in the direction of fixation is the same and equal to r , leading to the independence of the fixation probability on the degree of connectivity. The fixation dynamics, however, is accelerated because there are more ways to reach the final state of fixation. Similarly, for the specific spatial structure (fixed l) increasing the

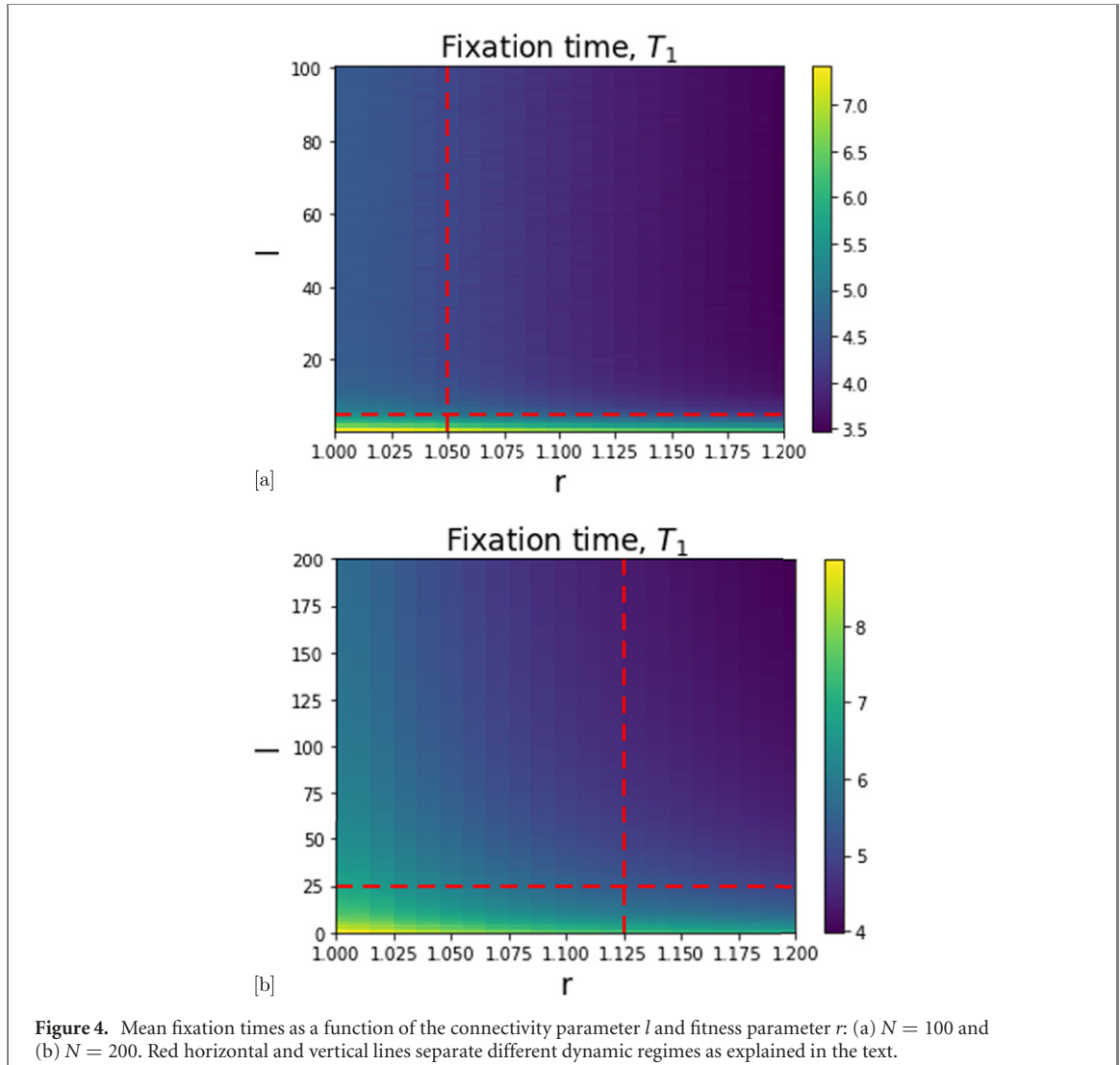


Figure 4. Mean fixation times as a function of the connectivity parameter l and fitness parameter r : (a) $N = 100$ and (b) $N = 200$. Red horizontal and vertical lines separate different dynamic regimes as explained in the text.

fitness for the mutated cells accelerates the fixation dynamics. This can be easily explained by the fact that for larger r the system reaches faster the fixation because of the larger bias.

The results for mean fixation times also indicate that there is a critical value of the connectivity parameter $l = l_c$ above which the dynamics becomes independent of l : see right upper rectangles in figure 4. This can be explained by again invoking the discrete-state stochastic scheme in figure 2(b). The last step before the mutation fixation is the transition from the state $N - 1$ to the state N with the rate a_{N-1} . It can be argued that for all possible values of l and N we have $a_{N-1} = r$. It seems that increasing the connectivity lowers the arrival time to the state $N - 1$, if the fitness parameter is large enough, making the transition $N - 1 \rightarrow N$ to be rate-limiting. Then the further increase in the parameter l will not affect the mean fixation time which will be mostly defined by the times to cross this rate-limiting step.

The main result of our theoretical analysis is that increasing the dimensionality of the cellular tissue from the effectively one dimensional to the effectively

three-dimensional accelerates the fixation dynamics. Since we have the explicit results for limiting spatial structures, the acceleration in the mutation fixation dynamics can be explicitly evaluated using equations (5), (10) and (11),

$$a = \frac{T_1(l=1)}{T_1(l=N-1)}. \quad (12)$$

Figure 5 exhibits the results of our theoretical calculations, and one can clearly see an almost linear dependence of the acceleration as a function of N . This is because for $N \gg 1$ the acceleration asymptotically behaves as $a \sim N/\ln(N)$ for $r > 1$, which for real tissues with $N \sim 10^5$ – 10^9 would translate into the acceleration $a \sim 10^4$ – 10^8 .

Our theoretical approach predicts that modifying the spatial structures of the tissues might strongly influence the cancer initiation dynamics. This is because changing the number of neighboring cells that can be affected after the cell division at the given cell modifies the dynamics of stochastic processes in the system that might lead to mutation fixation. Importantly, this provides a specific mechanism of

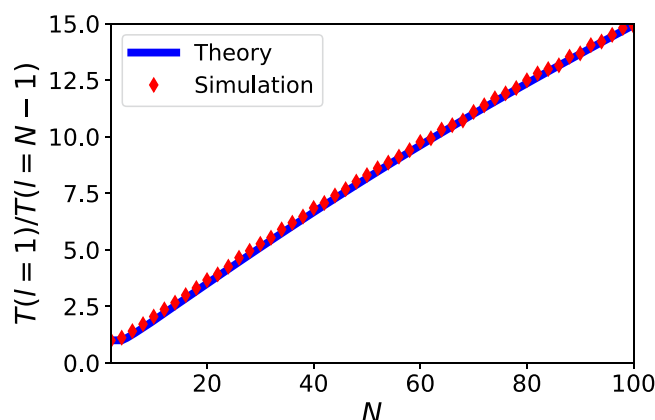


Figure 5. The ratio of fixation times versus N .

how tissue might lower the risks of tumor formation. We suggest that the nature could tune the tissue spatial structure via different regulation mechanisms to significantly delay the times of the tumor formation.

3. Summary and conclusions

In this paper, we presented a theoretical investigation on the role of tissue spatial structures in the formation of tumors. In our approach, the tissue is considered as network of cells and different spatial structures are mimicked by varying the connectivity in this network. By employing a Moran process on graph to evaluate the evolutionary dynamics in tissues, we evaluated the dynamics of the mutation fixation in the system where after the single mutation appearance only cell replications and removals are taking place. For our specific calculations, we mapped the transformations in the tissue to a set of stochastic transitions between different cellular states of the tissue. A method of first-passage processes was utilized then to explicitly evaluate the fixation probabilities and fixation times for different spatial arrangements and different rates of replications of the mutated cells. Our calculations show that for homogeneous tissues varying the spatial structures does not affect the fixation probability, while a strong effect is observed for the mean fixation times. The slowest fixation dynamics is observed for effectively one-dimensional tissues, while the fastest fixation dynamics is predicted for the effectively three-dimensional well-mixed tissues. It is also found that there is a critical connectivity parameter that separates two different dynamic regimes: in one of them the fixation dynamics depends on the spatial structures and in another one it becomes independent of the spatial details. These theoretical results are explained using the effective discrete-state stochastic schemes for underlying processes. Based on these results, it is argued how specifically tissues might minimize the danger of the cancer. We predict that varying the spatial structure will not decrease the probability of cancer, but it might significantly

increase the times when the tumor forms. Our theoretical analysis provides new insights on the microscopic origin of complex phenomena associated with the appearance of cancer in healthy tissues.

Although our theoretical method provides a physically reasonable approach to quantitatively evaluate the danger of cancer initiation, it is important to discuss its limitations and potential extensions. Our strongest simplification is that the tissue is fully homogeneous and all cells are identical. In real systems, heterogeneity is one of the main hallmarks of normal cellular tissues. It will be important to take into account this effect. A possible way to do it is to consider graphs with more complex topology and with non-uniform connectivity parameters [26]. Another assumption in our theoretical study is that the fitness parameter r is always constant, while in more realistic systems one could expect that r might change with time due to the accumulation of physiological changes in the system with increasing the number of mutated cells. In addition, we do not discuss the microscopic origins of connectivity, i.e., why the specific changes in the given cell (chemical, mechanical, etc) due to the cell division will force the removal of other specific cells. It is important to note that cell-cell interactions play an important role in the development of tumors [39]. It will be interesting to explore these and other possibilities in more advanced theoretical investigations of cancer initiation processes.

Author contributions

ABK designed the research; CS, HT and ABK performed the research; HT and ABK wrote the manuscript.

Funding statement

The work was supported by the Welch Foundation (C-1559), by the NSF (CHE-1953453 and MCB-

1941106), and by the Center for Theoretical Biological Physics sponsored by the NSF (PHY-2019745).

Data availability statement

All data that support the findings of this study are included within the article (and any supplementary files).

ORCID iDs

Hamid Teimouri  <https://orcid.org/0000-0002-3319-1187>

Anatoly B Kolomeisky  <https://orcid.org/0001-5677-6690>

References

- [1] Weinberg R A 2013 *The Biology of Cancer* (New York: Garland Science)
- [2] Hanahan D and Weinberg R A 2000 The hallmarks of cancer *Cell* **100** 57–70
- [3] Lodish H *et al* 2008 *Molecular Cell Biology* (London: Macmillan)
- [4] Vogelstein B, Papadopoulos N, Velculescu V E, Zhou S, Diaz L A and Kinzler K W 2013 Cancer genome landscapes *Science* **339** 1546–58
- [5] Hassler M R and Egger G 2012 Epigenomics of cancer—emerging new concepts *Biochimie* **94** 2219–30
- [6] Tomasetti C and Vogelstein B 2015 Variation in cancer risk among tissues can be explained by the number of stem cell divisions *Science* **347** 78–81
- [7] Jaffe N 2009 Osteosarcoma: review of the past, impact on the future *The American Experience. Pediatric and Adolescent Osteosarcoma* (New York: Springer) pp 239–62
- [8] Nowak M A, Michor F and Iwasa Y 2003 The linear process of somatic evolution *Proc. Natl Acad. Sci. USA* **100** 14966–9
- [9] Bozic I and Nowak M A 2013 Unwanted evolution *Science* **342** 938–9
- [10] Hindersin L and Traulsen A 2014 Counterintuitive properties of the fixation time in network-structured populations *J. R. Soc. Interface* **11** 20140606
- [11] Komarova N L and Myint P C 2006 Epithelial tissue architecture protects against cancer *Math. Biosci.* **200** 90–117
- [12] Almagro J, Messal H A, Elosegui-Artola A, van Rheenen J and Behrens A 2022 Tissue architecture in tumor initiation and progression *Trends Cancer* **8** 494
- [13] Martens E A, Kostadinov R, Maley C C and Hallatschek O 2011 Spatial structure increases the waiting time for cancer *New J. Phys.* **13** 115014
- [14] West J, Schenck R O, Gatenbee C, Robertson-Tessi M and Anderson A R 2021 Normal tissue architecture determines the evolutionary course of cancer *Nat. Commun.* **12** 1–9
- [15] Nowak M A 2006 *Evolutionary Dynamics: Exploring the Equations of Life* (Cambridge, MA: Harvard University Press)
- [16] Michor F, Nowak M A, Frank S A and Iwasa Y 2003 Stochastic elimination of cancer cells *Proc. R. Soc. London B* **270** 2017–24
- [17] Dominik W and Natalia K 2014 *Dynamics of Cancer: Mathematical Foundations of Oncology* (Singapore: World Scientific)
- [18] Foo J, Leder K and Michor F 2011 Stochastic dynamics of cancer initiation *Phys. Biol.* **8** 015002
- [19] Komarova N L, Sengupta A and Nowak M A 2003 Mutation-selection networks of cancer initiation: tumor suppressor genes and chromosomal instability *J. Theor. Biol.* **223** 433–50
- [20] Iwasa Y, Michor F and Nowak M A 2004 Evolutionary dynamics of invasion and escape *J. Theor. Biol.* **226** 205–14
- [21] Paterson C, Clevers H and Bozic I 2020 Mathematical model of colorectal cancer initiation *Proc. Natl. Acad. Sci. USA* **117** 20681–8
- [22] Teimouri H, Kochugavaeva M P and Kolomeisky A B 2019 Elucidating the correlations between cancer initiation times and lifetime cancer risks *Sci. Rep.* **9** 1–8
- [23] Teimouri H and Kolomeisky A B 2021 Temporal order of mutations influences cancer initiation dynamics *Phys. Biol.* **18** 056002
- [24] Teimouri H and Kolomeisky A B 2022 Can we understand the mechanisms of tumor formation by analyzing dynamics of cancer initiation? *Europhys. Lett.* **137** 27001
- [25] Tkadlec J, Pavlogiannis A, Chatterjee K and Nowak M A 2020 Limits on amplifiers of natural selection under death–birth updating *PLoS Comput. Biol.* **16** e1007494
- [26] Lieberman E, Hauert C and Nowak M A 2005 Evolutionary dynamics on graphs *Nature* **433** 312–6
- [27] Allen B, Sample C, Steinhagen P, Shapiro J, King M, Hedspeeth T and Goncalves M 2021 Fixation probabilities in graph-structured populations under weak selection *PLoS Comput. Biol.* **17** e1008695
- [28] Marrec L, Lamberti I and Bitbol A-F 2021 Toward a universal model for spatially structured populations *Phys. Rev. Lett.* **127** 218102
- [29] Frean M, Rainey P B and Traulsen A 2013 The effect of population structure on the rate of evolution *Proc. R. Soc. B.* **280** 20130211
- [30] Hindersin L, Werner B, Dingli D and Traulsen A 2016 Should tissue structure suppress or amplify selection to minimize cancer risk? *Biology Direct* **11** 1–11
- [31] Möller M, Hindersin L and Traulsen A 2019 Exploring and mapping the universe of evolutionary graphs identifies structural properties affecting fixation probability and time *Commun. Biol.* **2** 1–9
- [32] Orr H A 2005 The genetic theory of adaptation: a brief history *Nat. Rev. Genet.* **6** 119–27
- [33] Lynch M 2010 Rate, molecular spectrum, and consequences of human mutation *Proc. Natl. Acad. Sci. USA* **107** 961–8
- [34] Gillespie J H 1984 Molecular evolution over the mutational landscape *Evolution* **38** 1116–29
- [35] Huntly B J P *et al* 2004 MOZ-TIF2, but not BCR-ABL, confers properties of leukemic stem cells to committed murine hematopoietic progenitors *Cancer Cell* **6** 587–96
- [36] Redner S 2001 *A Guide to First-Passage Processes* (Cambridge: Cambridge University Press)
- [37] Kolomeisky A B 2015 *Motor Proteins and Molecular Motors* (Boca Raton, FL: CRC Press)
- [38] Lee-Six H *et al* 2018 Population dynamics of normal human blood inferred from somatic mutations *Nature* **561** 473–8
- [39] Li C 2017 Identifying the optimal anticancer targets from the landscape of a cancer-immunity interaction network *Phys. Chem. Chem. Phys.* **19** 7642–51